July 2002

ELSEVIER

Materials Letters 55 (2002) 182–188

MATERIALS LETTERS

www.elsevier.com/locate/matlet

Growth of Ni nanomagnetic particles in AlMCM41 host

Jin-Seung Jung [a,*], Sung Han Lee [b], Yong-Rok Kim [b], Leszek Malkinski [c], C.J. O'Connor [c,*]

[a] *Department of Chemistry, Kangnung National University, Kangnung, 210-702, South Korea*
[b] *Department of Chemistry, Yonsei University, Seoul, 120-749, South Korea*
[c] *Advanced Materials Research Institute, University of New Orleans, New Orleans, LA 70148, USA*

Received 20 August 2001; accepted 4 October 2001

Abstract

Nickel nanoparticles in AlMCM41 were prepared by the ion exchange and the reduction with H_2 gas. Annealing studies were carried out on Ni–AlMCM41 for the better understanding of the morphology, and magnetic properties of nickel nanoparticles depended on the annealing temperature. Products were characterized by transmission electron microscopy (TEM), X-ray powder diffraction (XRD), thermogravimetric analysis (TGA), and SQUID measurements.

Keywords: Nickel nanoparticles; AlMCM41; Annealing process; TEM; XRD; Magnetic properties

1. Introduction

There has been an increasing interest in the synthesis of ferromagnetic transition metal nanoparticles in terms of their fundamental importance as well as the potential application in magnetic recording technology [1–3]. Among the physical and chemical methods devised for the preparation of nanosized magnetic material, syntheses from non-magnetic inorganic matrix as a host have attracted attention as they can provide an effective way for tailoring a uniform particle size and prevent agglomeration of the particles in particle distribution [4]. Recently, porous materials attract much attention as the templates for making nanosized materials, as well as catalysts [5,6]. In 1992, researchers at Mobil synthesized a new family of mesoporous materials known as the M41S [7]. These have a good hexagonal array of one dimensional pores and a variable diameter of the pores. Therefore, the use of a mesoporous AlMCM41 silica tube offers excellent control of the particle dimension compared to the ion-exchange polymer resins and sol–gel derived oxide matrices [8,9]. Recently, we have started a research aimed to the preparation and characterization of nanomagnetic metals dispersed in an AlMCM41 [10–12]. We have reported that the nickel nanoparticles in AlMCM41 can be obtained during the reduction after the insertion of nickel cations into AlMCM41 [10]. We have also described that the nickel particle size and blocking temperature depend on the reduction method [12]. However, these

* Corresponding authors. J.-S. Jung is to be contacted at Tel.: 82-33-640-2305; fax: 82-33-640-2738. C.J. O'Connor, Tel.: +1-504-280-6840; fax: +1-504-280-3185.

E-mail addresses: jjscm@kangnung.ac.kr (J.-S. Jung), coconnor@uno.edu (C.J. O'Connor).

0167-577X/02/$ - see front matter
PII: S0167-577X(01)00643-7

materials have the blocking temperature lower than the room temperature owing to small particle size. In this paper, we have annealed at different temperatures for better understanding of the morphology and magnetism of nickel nanoparticles in AlMCM41 host.

2. Experimental section

2.1. Synthesis

Ni^{2+}–AlMCM41 was prepared by the previously reported method [10]. The reduction of Ni^{2+}–

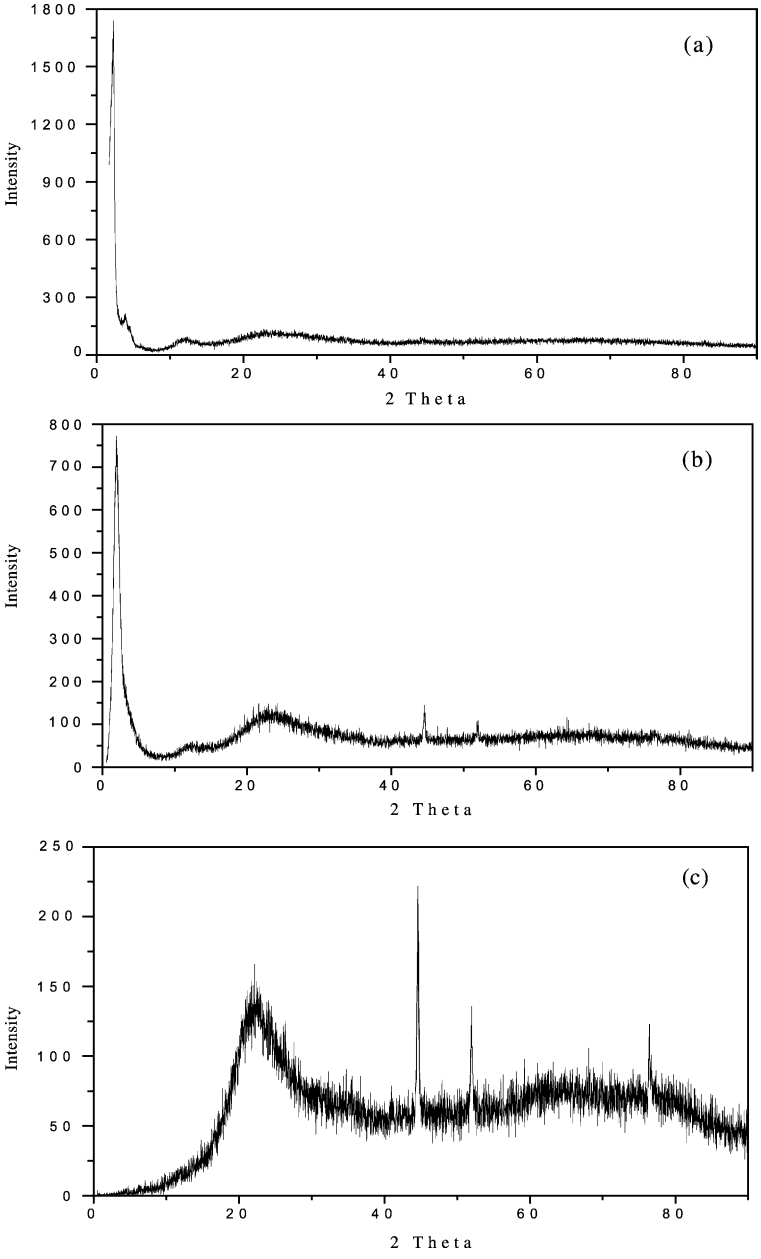

Fig. 1. XRD pattern of Ni–AlMCM41: (a) as-reduced at 450 °C, (b) after annealing at 600 °C, (c) after annealing at 800 °C.

AlMCM41, which was prepared from H_2-N_2 (4/96 v/v%) gas mixture at 450 °C for 3 h. In order to avoid any possible oxidation of the nickel particles, the samples were prepared in a glove box under an argon atmosphere. Annealing studies were carried out on Ni–AlMCM41 to gauge its effect on both the host and the nickel metal particles. Samples were heated at 600 and 800 °C in sealed evacuated ($<10^{-3}$ Torr) pyrex tubes for 8 h.

2.2. X-ray diffraction

X-ray powder diffraction (XRD) data were collected on a Philips X-Pert MPD system equipped with copper radiation ($2\theta = 1.5418$ Å) and a graphite monochrometer.

2.3. Transmission electron microscopy (TEM)

Samples were ultrasonically dispersed in acetone and a drop of the suspension was deposited on a holey carbon copper grid. Micrographs were taken on a JEOL 2010 microscope operated at 200 kV.

2.4. Magnetic measurements

The magnetic properties of the Ni–AlMCM41 were characterized using a Quantum Design Model MPMS-5S SQUID susceptometer. Calibration and measurement procedures have been described in detail elsewhere [13]. Two types of magnetic measurements were conducted: dc magnetic susceptibility, both field-cooling (FC) and zero-field-cooling (ZFC), as a function of temperature down to 1.7 K and magnetization as a function of field or temperature.

2.5. Thermogravimetric analysis (TGA)

TGA was performed on a TA-2050 analyzer. The samples were heated for TG measurements in an air flow of 55 ml/min at a heating rate of 5 °C/min.

3. Results and discussion

The XRD pattern obtained after the reduction with hydrogen at 450 °C did not show the existence of nickel particles but maintained the host framework during the formation process of nickel clusters (Fig. 1(a)). However, the peaks corresponding to nickel began to appear upon annealing the reduction products at 600 °C in sealed evacuated pyrex tubes for 8 h. Furthermore, the host framework began to collapse around 600 °C (Fig. 1(b)) and was completely collapsed at 800 °C (Fig. 1(c)). FCC characteristic peaks of elemental nickel showed the amorphous to crystalline transformation of the inserted nickel. Previ-

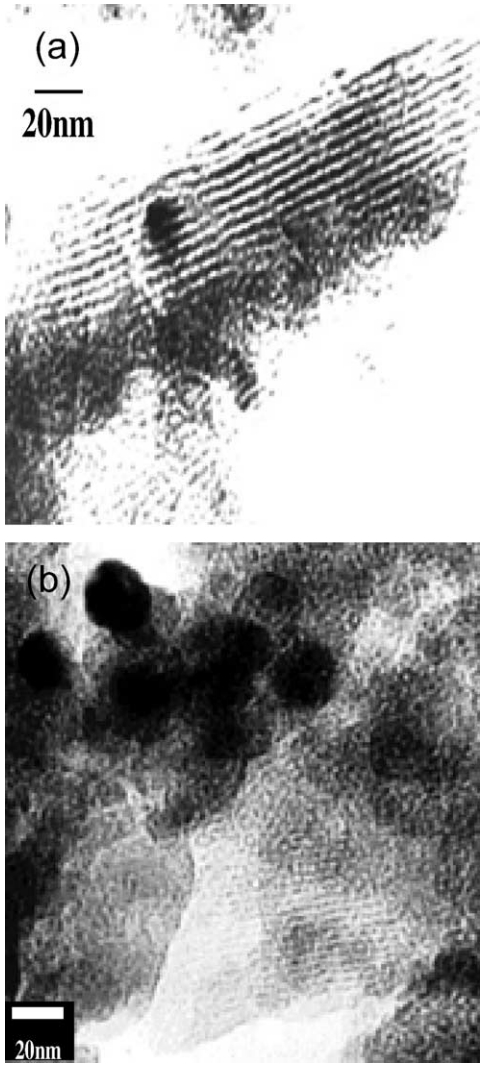

Fig. 2. TEM image of Ni–AlMCM41: (a) lamellar structure from the projection of a hexagonal of tubules, (b) after annealing at 600 °C.

ously, we reported the TEM images of a lamellar structure and honeycomb structure for the as-reduced product. In these micrographs, host structure can clearly be observed, but the image of inserted nickels cannot be found owing to the little contrast between the pore spaces and the nickel particles (Fig. 2(a)). Fig. 2(b) shows the TEM micrographs of the Ni–AlMCM41 after annealing at 600 °C. This shows parallel pattern to the pore direction and also the nickel clusters on the external surfaces. This is probably due to the fact that nickel particles show that grain growth depends on the collapse of host framework. Thermogravimetric analysis of the host AlMCM41 and Ni–AlMCM41 (Fig. 3) was performed in air atmosphere. Three distinct stages were observed in the thermogram of the host AlMCM41, first desorbs molecular water at 25–150 °C, second is related to the surfactant species at 25–400 °C, and the last one is water molecules from silanol groups condensate to form siloxane bonds at 400–600 °C. The TG curve of Ni–AlMCM41 is slightly decrease except annealed Ni–AlMCM41 after annealing at 800 °C (Fig. 3, inset). It is evident that the surface exposed nickel particles after the collapse of host AlMCM41, absorbed oxygen in air.

Comparison of the magnetization of the samples at the temperature of 2 K (Fig. 4(a)) with the saturation magnetization of pure Ni allows estimating the weight fraction of Ni particles in the MCM41 host of about 1.8%. This value is slightly larger than the previously reported one [10]. The fact that the hysteresis curves do not saturate at a low temperature as 2 K indicates that there is a significant fraction of very small particles in non annealed samples [14]. This conclusion can also be made based on the saturation magnetization at 300 K, which is almost one order of magnitude smaller than the low temperature value (Fig. 4). The particles reveal superparamagnetic properties with the blocking temperature T_B of about 240 K for as-reduced sample (Fig. 5(a)) and T_B above room temperature for the annealed sample (Fig. 5(b,c)). The increase of the blocking temperatures for the annealed samples is due to the increase of particles' size, which can be calculated about 30 nm from blocking temperature [15]. It is also been verified by the TEM images and

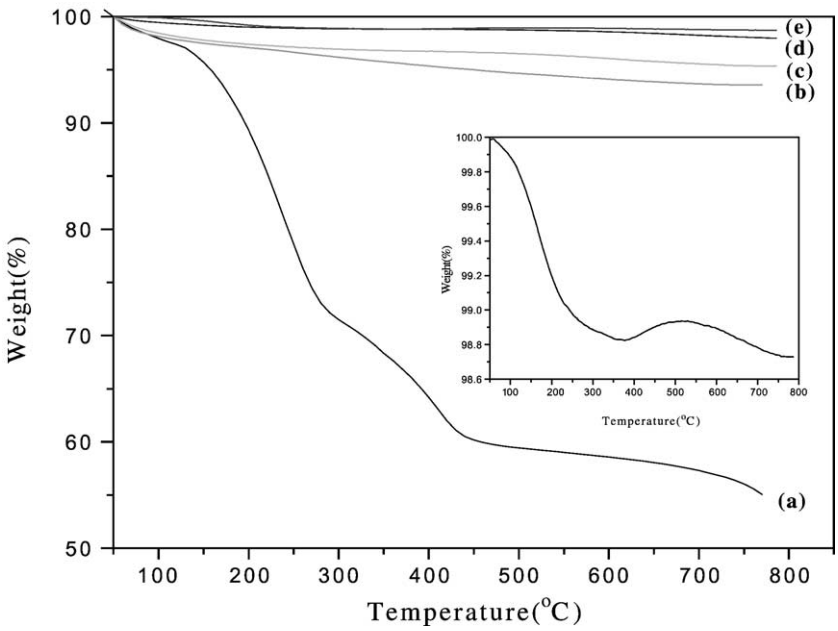

Fig. 3. Thermal analysis for (a) before calcination of AlMCM41, (b) after calcination of AlMCM41, (c) Ni–AlMCM41 (H_2 reduction at 450 °C), (d) Ni–AlMCM41 after annealing at 600 °C, (e) Ni–AlMCM41 after annealing at 800 °C.

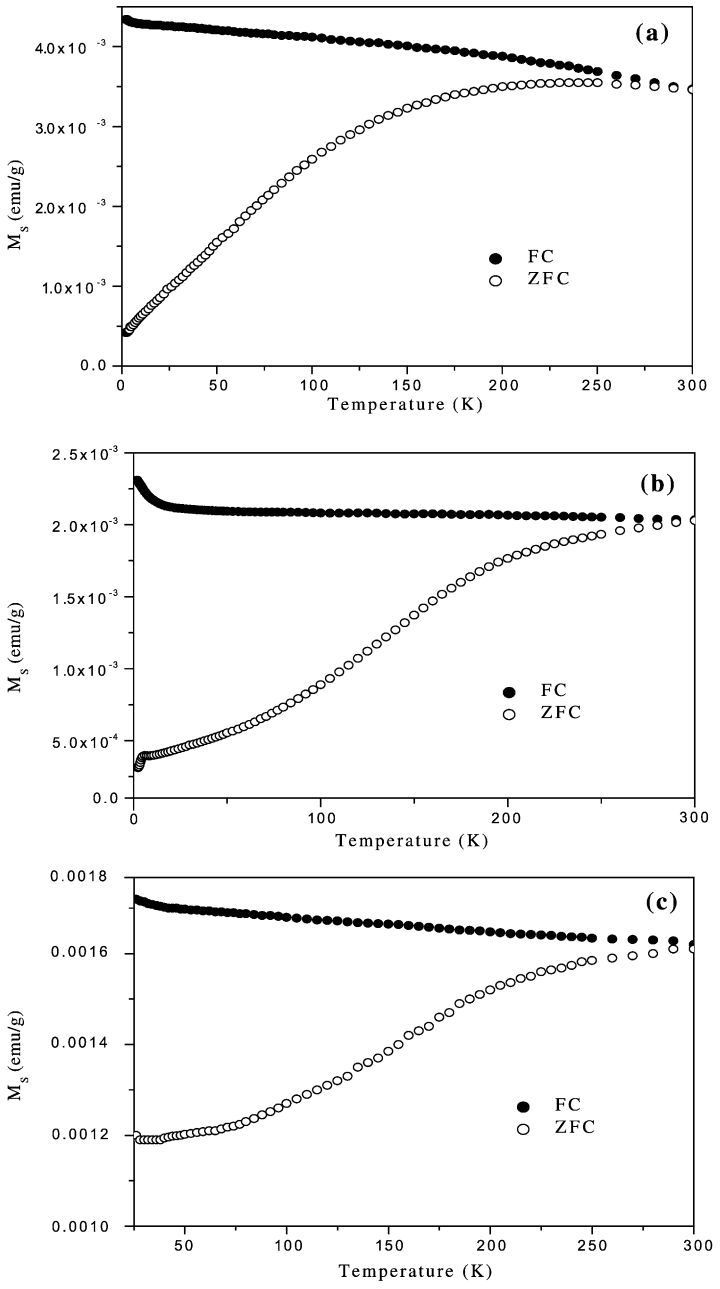

Fig. 4. Magnetic hysteresis loop of the Ni–AlMCM41 : (a) as-reduced at 450 °C, (b) after annealing at 600 °C, (c) after annealing at 800 °C.

Scherrer equation of the XRD peak [16]. The low temperature coercivity was 350, 450, and 240 Oe for as-reduced and annealing sample at 600, 800 °C, respectively.

4. Conclusions

Nanoparticle aggregations of nickel in an AlMCM41 have been prepared by the annealing of reduced

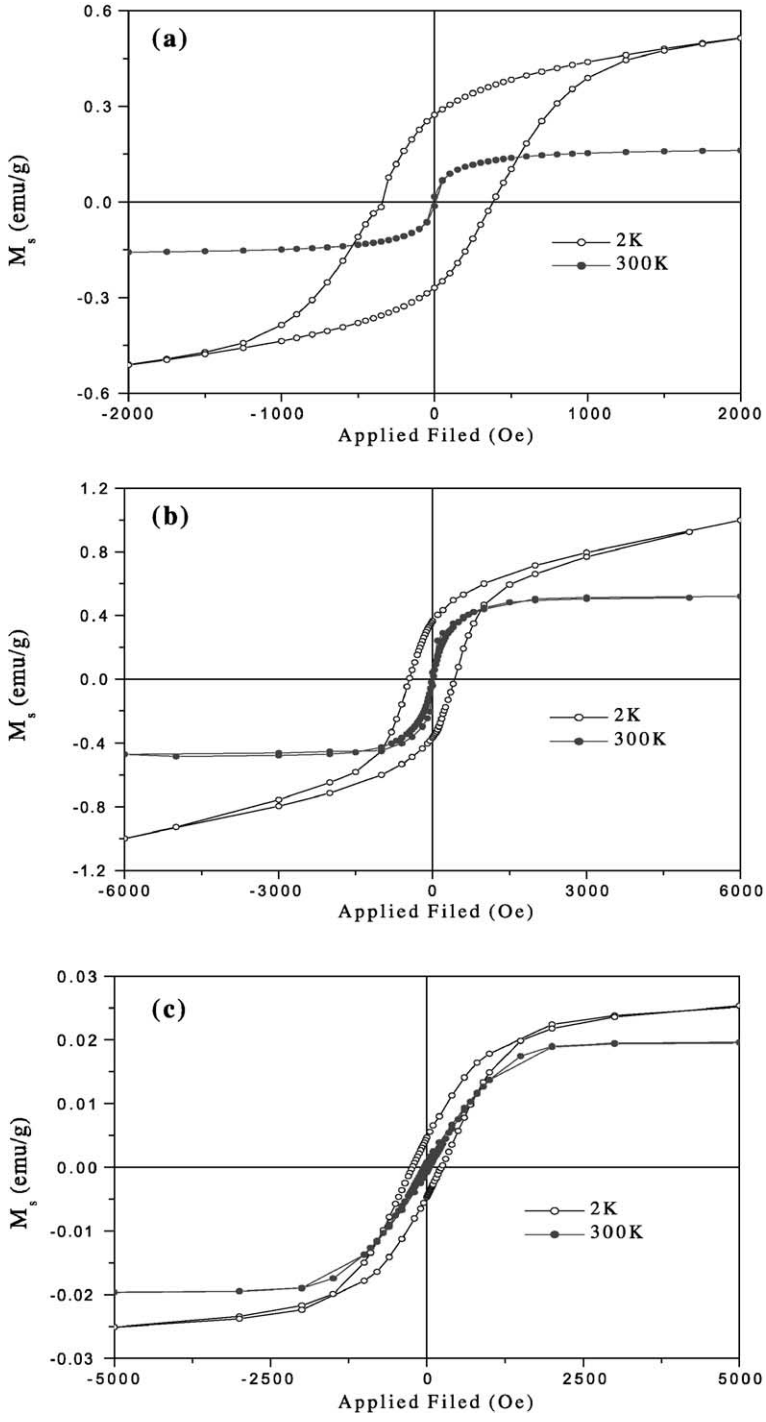

Fig. 5. Temperature dependence field-cooled (FC) and zero-field cooled (ZFC) dc magnetic susceptibilities of Ni–AlMCM41 (a) as-reduced at 450 °C, (b) after annealing at 600 °C, (c) after annealing at 800 °C.

Ni–AlMCM41. In the XRD work for the AlMCM41 stability and size of nickel particles, we measured the particles in the 600 and 800 °C annealing temperature as 30 and 35 nm and found completely collapsed at 800 °C. This is supported by TEM studies. The measure magnetism of annealed nickel particles shows superparamagnetism properties with blocking temperature over room temperature.

Acknowledgements

This work was supported by Grant No. KRF-2000-042-D00056 and by the US Department of Defense (DARPA MDA972-97-1-0003) and also by Myongji RRC.

References

[1] J.L. Dorman, Mater. Sci. Eng. 168 (1993) 217.
[2] C.L. Chien, Mater. Res. Soc. Symp. Proc. 195 (1990) 411.
[3] R.D. Shull, L.H. Bennett, Nanostruct. Mater. 1 (1992) 83.
[4] L. Zhang, G.C. Papaefthymiou, J.Y. Ying, J. Appl. Phys. 81 (1997) 6892.
[5] A. Corma, Chem. Rev. 97 (1997) 2373.
[6] T. Bein, C. Wu, Chem. Mater. 6 (1994) 1109.
[7] J.S. Beck, J.C. Vartuli, W.J. Roth, M.E. Leonowicz, C.J. Kresge, K.D. Schnitl, C.T.-W. Chu, K.H. Olson, E.W. Sheppard, S.B. McCullen, J.B. Higgins, J.L. Schlenken, J. Am. Chem. Soc. 114 (1992) 10834.
[8] R.D. Shull, J.J. Ritter, A. Shapiro, L.J. Swartzendruber, H.L. Bennett, J. Appl. Phys. 67 (1990) 4490.
[9] S. Roy, D. Das, D. Chakravorty, D.C. Agarwal, J. Appl. Phys. 74 (1993) 4746.
[10] J.-S. Jung, W.-S. Chae, R.A. McIntyre, C.T. Seip, J.B. Wiley, C.J. O'Connor, Mater. Res. Bull. 34 (1999) 1353.
[11] J.-S. Jung, J.-Y. Kim, W.-S. Chae, Y.-R. Kim, J.-H. Jun, L. Malkinski, M.L. Viciu, W. Zhou, J.B. Wiley, C.J. O'Connor, MRS Proc. (2001) 676.
[12] J.-S. Jung, K.-H. Choi, W.-S. Chae, Y.-R. Kim, J.-H. Jun, L. Malkinski, T. Kodenkandath, W. Zhou, J.B. Wiley, C.J. O'Connor, submitted for publication.
[13] C.J. O'Connor, Prog. Inorg. Chem. 29 (1982) 203.
[14] L.M. Malkinski, J.-Q. Wang, J. Dai, J. Tang, C.J. O'Connor, Appl. Phys. Lett. 75 (2000) 844.
[15] D.L. Leslie-Pelecky, R.D. Rieke, Chem. Mater. 8 (1996) 1770.
[16] D.L. Leslie-Pelecky, X.Q. Zhang, S.H. Kim, M. Bonder, R.D. Rieke, Chem. Mater. 10 (1998) 164.